Carbohydrate Polymers 151 (2016) 760–769

Contents lists available at ScienceDirect

Carbohydrate Polymers

journal homepage: www.elsevier.com/locate/carbpol

Fast ultrasound assisted synthesis of chitosan-based magnetite nanocomposites as a modified electrode sensor

T.M. Freire[a], L.M.U. Dutra[b,d], D.C. Queiroz[b], N.M.P.S. Ricardo[b], K. Barreto[b], J.C. Denardin[c], Frederik R. Wurm[d], C.P. Sousa[e], A.N. Correia[e], P de Lima-Neto[e], P.B.A. Fechine[a,*]

[a] Group of Chemistry of Advanced Materials (GQMAT)-Department of Analytical Chemistry and Physical-Chemistry, Federal University of Ceará-UFC, Campus do Pici, CP 12100, CEP 60451-970 Fortaleza, CE, Brazil
[b] Department of Organic and Inorganic Chemistry, Federal University of Ceará-UFC, Campus do Pici, CP 12100, CEP 60451-970 Fortaleza, CE, Brazil
[c] Department of Physical, University of Santiago de Chile, USACH, Av. Ecuador 3493, Santiago, Chile
[d] Max Planck Institute for Polymer Research, Ackermannweg 10, 55128 Mainz, Germany
[e] Group of Electrochemistry and Corrosion (GELCORR)-Department of Analytical Chemistry and Physical-Chemistry, Federal University of Ceará-UFC, Campus do Pici, CP 12100, CEP 60451-970 Fortaleza, CE, Brazil

ARTICLE INFO

Article history:
Received 28 January 2016
Received in revised form 25 May 2016
Accepted 26 May 2016
Available online 3 June 2016

Keywords:
Nanocomposites
Magnetite
Chitosan
Superparamagnetic
Ultrasound

ABSTRACT

Chitosan-based magnetite nanocomposites were synthesized using a versatile ultrasound assisted *in situ* method involving one quick step. This synthetic route approach results in the formation of spheroidal nanoparticles (Fe_3O_4) with average diameter between 10 and 24 nm, which were found to be superparamagnetic with saturation magnetization (Ms) ranges from 32–57 emu g^{-1}, depending on the concentration. The incorporation of Fe_3O_4 into chitosan matrix was also confirmed by FTIR and TG techniques. This hybrid nanocomposite has the potential application as electrochemical sensors, since the electrochemical signal was excepitionally stable. In addition, the *in situ* strategy proposed in this work allowed us to synthesize the nanocomposite system in a short time, around 2 min of time-consuming, showing great potential to replace convencional methods. Herein, the procedure will permit a further diversity of applications into nanocomposite materials engineering.

1. Introduction

Development of organic-inorganic nanocomposites has attracted attention of many researchers, since these materials can be applied in different areas of science. Magnetic nanoparticles (MNPs), such as magnetite (Fe_3O_4), have shown huge potential for different applications: enzyme immobilization, waste water treatment, targeted delivery of drugs and biosensors (Lim et al., 2015; Wang, Li, Luo, Wang, & Duan, 2016; Zhang et al., 2010), owing to their superparamagnetic behavior and low toxicity. However, the large surface area-to-volume ratio in Fe_3O_4 MNPs exhibits a high surface energy and they tend to aggregate, limiting their range of applications (Gregorio-Jauregui et al., 2012; Yallapu et al., 2011).

Herein, controlling and/or preventing particles agglomeration makes their production a truly challenge into industry field. Thus, organic compounds have been used to cover MNPs, promoting stability and surface functionalization (Nicolás et al., 2013; Zhang et al., 2012). Several works proved that magnetite nanoparticles coated by chitosan (Shete et al., 2014), poly(vinyl alcohol) (Mahmoudi, Simchi, & Imani, 2009), poly(acrylic acid) (Xu, Zhuang, Lin, Shen, & Li, 2013), DNA (Navarathne, Ner, Jain, Grote, & Sotzing, 2011), or proteins (Bayrakci et al., 2014Bayrakci, Gezici, Bas, Ozmen, & Maltas, 2014), promotes whether electrostatic or steric repulsion, stabilizing MNPs dispersion. Chitosan has become one of most used natural polymer, being biocompatible, biodegradable and bioactive. Additionally, this polyaminosaccharide has intrinsic chemical properties, which its free amino groups allow the formation of positively charged complexes, providing reactive sites to bind Fe-based MNPs (Shen, Shen, Wen, Wang, & Liu, 2011; Zhang et al., 2010).

Some studies have been demonstrated that nanosize and surface effects display significant rules in NP's magnetic behavior.

* Corresponding author.
E-mail addresses: tiagomfreire.ufc@gmail.com (T.M. Freire), lmudutra@hotmail.com (L.M.U. Dutra), daniloqueiroz46@gmail.com (D.C. Queiroz), nagilaricardo@gmail.com (N.M.P.S. Ricardo), kambarreto@yahoo.com.br (K. Barreto), juliano.denardin@usach.cl (J.C. Denardin), wurm@mpip-mainz.mpg.de (F.R. Wurm), pinheiro.cs@gmail.com (C.P. Sousa), adriana@ufc.br (A.N. Correia), pln@ufc.br (P. de Lima-Neto), fechine@ufc.br (P.B.A. Fechine).

http://dx.doi.org/10.1016/j.carbpol.2016.05.095
0144-8617/

Innumerous strategies have been developed in order to modulate a hybrid functional metal oxide with desired properties, such as co-precipitation (Silva et al., 2013), hydrothermal synthesis (Gyergyek, Drofenik, & Makovec, 2012) and sonochemistry (Barkade, Pinjari, Nakate et al., 2013; Barkade, Pinjari, Singh et al., 2013; Theerdhala et al., 2010). However, these methods are energy and time-consuming, and thus it is important to highlight the use of ultrasound for synthesis involving a wide range of nanomaterials, such as silver nanoparticles (He et al., 2014), magnesium ferrite (Chen, Li, zhang, & Kang, 2013) and iron oxide (Dolores, Raquel, & Adianez, 2015). The technique has become an easy and simple tool, that may promotes ultrahigh surface area (organic/inorganic) with synthesis of inorganic material during process (*in situ* method), which the formation of a monodisperse can tailor hybrid materials, controlling the crystal growth and forming particles with nanometer size distribution (Barkade, Pinjari, Singh et al., 2013; Carroll, Ulises-Reveles, Shultz, Khanna, & Carpenter, 2011).

In general, chitosan-based magnetite synthesis results in two types of different structures: a single magnetite core surrounded by a chitosan layer, and/or magnetite "multi-cores" dispersed in a chitosan matrix (Patil et al., 2014; Reddy & Lee, 2013; Safari & Javadian, 2015). Recently, Safari and Javadian synthesized Fe_3O_4-chitosan nanoparticles by co-precipitation method under ultrasound irradiation in two different steps. Firstly, they obtained the magnetic nanoparticles by chemical co-precipitation, followed by a subsequent functionalization with chitosan by aid of ultrasound. Even though, cavitation phenomenon provides an increase in reactions rate, the ultrasound irradiation (US) is used only in the second step. Thereby, the adapted method is still being time-consuming, since the synthesis is carried out in two sequential steps, namely particle precipitation and functionalization (Safari & Javadian, 2015).

In this work, we present a rapid ultrasonic assisted *in situ* route to produce magnetic Fe_3O_4-chitosan nanocomposites, where the chemical co-precipitation and functionalization occur at the same time, *i.e.*, in one quick step. Besides the *in situ* method synthesizes MNPs with low crystallite size, high crystallinity and saturation magnetization, the nanocomposite material has shown optimal electrochemical response due to development of modified electrodes. Furthermore, our method minimizes the oxidation of magnetite and drastically decreases the synthesis time from several minutes and/or hours for the conventional co-precipitation method to a few minutes (~2 min). Additionally, in the sense of electrochemical sensors application, the proposed route is potentially ideal to produce a large amount of material, *i.e.*, scaling up to industrial level, since sensors of hybrid materials based on chitosan and Fe_3O_4 have been developed for detection of glucose (Kaushik et al., 2008), urea (Kaushik et al., 2009) and as sensors for diseases diagnosis (Tran et al., 2011).

2. Experimental procedure

2.1. Materials

Chitosan (DPN – Delta Produtos Naturais Ltda) was characterized regarding to molecular weight (M_w), 31 kDa, and deacetylation degree (DD), 92%, by gel permeation chromatography (GPC) and potenciometry, respectively. Ferric chloride hexahydrate ($FeCl_3{\cdot}6H_2O$, 97%), potassium ferrocyanide ($K_4Fe(CN)_6$, 98.5%), potassium ferricyanide ($K_3Fe(CN)_6$, 99%), potassium chloride (KCl, 99%) and glacial acetic acid (CH_3COOH, 99.7%) were purchased from VETEC. Ferrous sulfate heptahydrate ($FeSO_4{\cdot}7H_2O$, 99%) and ammonium hydroxide solution (NH_4OH, 30%) were purchased from DINAMICA, and glutaraldehyde solution 25% from Sigma-Aldrich. All used reagents are analytical grade.

2.2. Preparation of chitosan/Fe_3O_4 nanocomposites

The magnetic chitosan nanocomposites were synthesized as follow. Firstly, different amounts of chitosan (0.1, 0.05 and 0.01 g) were dissolved in 15 mL of acetic acid 1% (v/v) under stirring at 50 °C for 10 min. Subsequently, 10 mL of Fe solution 0.33 mol L^{-1} ($FeCl_3.6H_2O/FeSO_4.7H_2OFeCl_3{\cdot}6H_2O/FeSO_4{\cdot}7H_2O$ (Fe^{3+}:Fe^{2+}, 2:1 molar ratio) was added into chitosan solutions. After homogenization, 2 mL of NH_4OH was slowly added under US irradiation for 2 min (50% amplitude, in a pulse regime 20 s *on*–10 s *off*) using a G. Heinemann Ultraschall – und Labor techinik Sonifier. The resultant precipitated chitosan-based magnetite was removed from the solution by magnetic decantation. Then, obtained chitosan/Fe_3O_4 nanoparticles were washed several times with distilled water and redispersed in a glutaraldehyde (GL) solution (chitosan: GL, 2:1 molar ratio) at 50 °C for 2 h under mechanical stirring. The final product was washed several times with distilled water and dried in an oven at 50 °C for 48 h. The samples were collected as a black powder and labeled as ChM 0.1, ChM 0.05 and ChM 0.01, where the numbers 0.1, 0.05 and 0.01 correspond to the mass of chitosan used in the synthesis. The same strategy was used in the synthesis of "naked" Fe_3O_4 nanoparticles.

2.3. Characterization methods

X-ray Powder Diffraction (XRPD) analysis was performed to confirm the crystalline structures of magnetite present in chitosan/Fe_3O_4 nanocomposites. The samples were analyzed by X-ray powder diffractometer Xpert Pro MPD (Panalytical) using Bragg–Brentano geometry in the range of 15°–70° with a rate of 1° min^{-1}. CuKα radiation (k = 1.54059 Å) was used and the tube operated at 40 kV and 30 mA.

Fourier Transform Infrared Spectroscopy (FTIR) analysis was carried out in a PerkinElmer 2000 spectrophotometer used to record spectra in the range between 4000 and 400 cm^{-1}. Previously measurements, the samples were dried and grounded to powder and pressed (~10 mg of sample to 100 mg of KBr) in disk format.

The morphologic study was performed by Transmission Electron Microscopy (TEM). The images were recorded by using a JEOL JEM-1400 electron microscope operating at an accelerating voltage of 120 kV. The samples were prepared by diluting nanoparticles dispersion in distillated water. Then, one droplet of the sample was placed on 300 mesh carbon-coated cooper grids and dried overnight under ambient conditions. The size distribution was determined by measurement of 50 randomly selected particles in different regions of the expanding TEM image.

For thermogravimetric analysis (TG), 5 mg of nanoparticles were carried out in nitrogen atmosphere by employing a Thermogravimetric Analyzer Q50 V20. The loss of mass was monitored heating up samples from 25 to 900 °C in a rate of 10 °C min^{-1}. The zero time for the thermal degradation study was taken after temperature stabilization.

Magnetic properties were investigated by a Vibrating Sample Magnetometer (VSM) Mini 5 T from Cryogenic Ltd. Previously, the VSM was calibrated using a YIG sphere, and after measuring the mass of each sample, the magnetization was given in emu g^{-1}. The zero-field-cooled (ZFC) curve was obtained by cooling the samples (300–5 K) in the absence of an external field, upon reaching temperature an external field is applied and measured as a function of the increasing temperature. The field-cooled (FC) curve is obtained following the same ZFC procedure; instead, the samples are cooled in the presence of external field.

Cyclic voltammetry measurements were carried out with a potentiostatic (Autolab PGSTAT 101 Metrohn- Eco Chemie) controlled by a personal computer with Nova version 1.11.2 software using conventional three-electrode system. This is composed by a

modified glassy carbon electrode (GCE) (3 mm of diameter, BASi) as the working electrode, a Pt sheet as auxiliary electrode and an $Ag_{(s)}/AgCl_{(s)}/Cl^{-}{}_{(aq)}$ (saturated KCl) as reference electrode. All measurements were performed in a solution of 1.0×10^{-3} mol L^{-1} $Fe(CN)_6{}^{3-/4-}$ containing 0.1 mol L^{-1} KCl in different scan rates. The GCE was carefully polished with 3 μm diamond paste and was ultrasonicated in ethanol and purified water. The modified GCE was prepared by adding a 5 μL of sample dispersion 1 mg mL^{-1} in Br buffer pH 6 onto the top of the electrode. The solvent was allowed to evaporate at room temperature (23 ±1 °C) for 60 min. When not in use, the modified electrode was stored in a desiccator at room temperature.

3. Results and discussion

3.1. Synthesis of chitosan/Fe_3O_4 nanocomposites

Chitosan-Fe_3O_4 nanocomposites have been prepared by chemical co-precipitation method under US irradiation. The procedure scheme and idealized obtained structure are shown in Fig. 1(a) and **(b)**, respectively. As previously described in Section 1, the work proposal to use ultrasound assisted *in situ* chemical co-preciptation method has several advantages over conventional procedures. Since, the synthesis is carrying out under US irradiation, the sonication waves themselves promote a homogenous dispersion with an ultrahigh surface area between chitosan and iron ions. In the first stage, Fe^{2+} and Fe^{3+} ions are captured by the amino groups of chitosan to form the chitosan-complexed Fe. As a result of this chelation effect, the chelated amino groups can hinder the iron ions diffusion, controlling the growth of magnetite crystals (Wang, Li, Zhou, & Jia, 2009). In the second stage, while the base is added, the cavitation process improves the system homogeneity, avoiding the formation of agglomerates during the crystal growth. The *in situ* magnetite mineralization under US irradiation can be observed in Eq. (1).

$$Fe^{2+} + 2Fe^{3+} + 8OH^{-} \xrightarrow{)))} Fe_3O_4 + 4H_2O \quad (1)$$

Ultrasound assisted methods have been an upsurge in the study of hybrid nanocomposites, owing to interesting properties (Patil et al., 2014; Reddy & Lee, 2013; Safari & Javadian, 2015; Shete et al., 2014). Generally, the magnetic nanoparticle (Fe_3O_4) is firstly synthesized, and chitosan matrix is formed subsequently. However, our methodology presents one quick step *in situ* synthesis to produce the chitosan/Fe_3O_4 nanocomposite, where the sonication time has an important role in the synthesis, as well as in final product properties. Since the procedure leads with chitosan during US irradiation, some limitations have to be considered, thereby to avoid some negative effects. For instance, during the pulse *on* the collapse of the bubbles provides a high shear force, occurring cleavage of chitosan molecules. In this work, even with a low pulse-time-regime of 2 min, the chitosan molecular weight (M_w) was checked after synthesis by GPC. As expected, the decrease of chitosan M_w was slightly significant, considering that the obtained M_w values are in the same range of chitosan before sonication step, 30–10 kDa for each chitosan solution (Ch 0.01, 0.05 and 0.1) (Wu, Zivanovic, Hayes, & Weiss, 2008). Another relevant point is the inhomogeneous output power, caused by the heating up of the probe, if the ultrasound is used for a long time. Besides the heating up of the probe may decrease the amplitude%, high temperatures provide oxidation of Fe(II) to Fe(III), decreasing substantially the saturation magnetization of the MNPs, may influence negatively in the superparamagnetic property, and also the efficiency of the synthesis.

Other point that should be considered is the reticulation step after the synthesis of the nanocomposite. For example, adsorbent and resin materials require biopolymers resistant to acidic medium, and that has a direct relation with crosslinking reactions. Considering a chitosan-based hybrid material, few studies have reported instability of chitosan in strongly acidic medium (Sinha et al., 2004). Thereby, crosslinker agents as glutaraldehyde have been used to stabilization purposes, forming Schiff base linkages, in which may acquire good stability to nanocomposites. Thus, producing a versatile and resistance chitosan-based magnetite under mild conditions, where it can be applied in different usages.

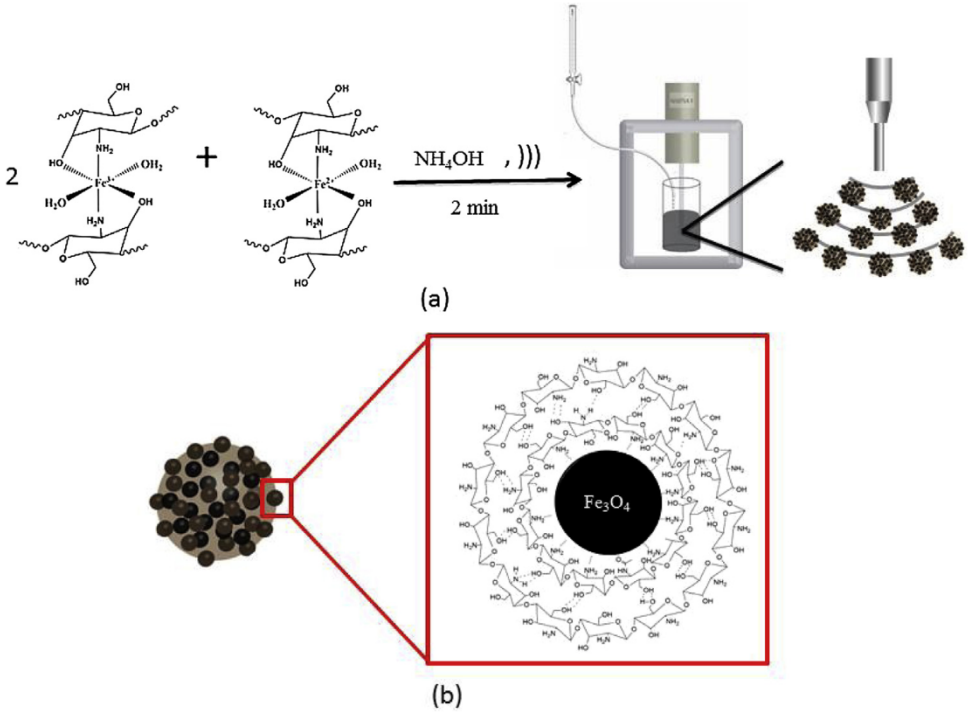

Fig. 1. (a) Schematic representation for the preparation of Fe_3O_4-chitosan nanocomposites by ultrasonication and (b) final structural arrangement.

3.2. Characterization of chitosan/Fe_3O_4 nanocomposites

3.2.1. Morphological and structural characterization

XRPD technique was used to identify the crystalline structure of the magnetic nanoparticles dispersed in chitosan matrix, as shown in Fig. 2(a). All samples presented main characteristic peaks at 30.2, 35.6, 43.2, 53.6, 57.2, 62.8°, which can be indexed to (220), (311), (400), (422), (511) and (440) planes, respectively, by comparison with inorganic crystal structure database (ICSD, file n° 01-086-1340). These peaks are associated with cubic spinel phase of magnetite (Fe_3O_4), and patterns peaks observed in all obtained nanocomposites showed the crystalline structure of magnetite. However, it was possible to observe that the sample ChM 0.1 presented the broadening at half the higher maximum intensity when compared to the other samples. This increasing may be associated with the influence of amorphous structure of chitosan. This influence was not observed in the ChM 0.05 and ChM 0.01 samples, suggesting that the interference of chitosan is only observed when the molar ratio of chitosan monomer and iron ions is higher than 0.1902.

All diffractograms were refined by using Rietveld method. The lattice parameters (a = b = c) for samples Fe_3O_4, ChM 0.01, ChM 0.05 and ChM 0.10 were found to be 8.3625, 8.3534, 8.3510 and 8.3517, respectively. These results indicate a strong interaction between chitosan and magnetite occasioned by contractions of the unit cell of magnetite. The crystallite size was calculated according to Scherrer's equation, which is represented as

$$T_c = \frac{K\lambda}{\beta cos\theta} \quad (2)$$

where T_c is the average diameter of crystallite; K is the dimensional factor; λ is the X-ray wavelength; β is the broadening at half of the maximum intensity and θ is the Bragg's angle. Diameter values of the samples Fe_3O_4, ChM 0.01, ChM 0.05 and ChM 0.1 were found to be 11.65 ± 0.11, 12.67 ± 0.10, 11.79 ± 0.16 and 8.37 ± 0.18 nm, respectively. Gregorio-Jauregui and coworkers obtained chitosan-based magnetite nanoparticles by co-precipitation method, which were mixed $FeCl_3 \cdot 6H_2O$ and $FeCl_2 \cdot 4H_2O$ with different chitosan mass in a reactor (Gregorio-Jauregui et al., 2012), and it was observed a crystallite size similar to found in this work. However, they used larger amount of chitosan and the synthesis is time-consuming, more than 30 min. Clearly, associated with the US irradiation, it is observed chitosan acting as a controller of the crystallite size, and that can be associated with the Fe-chitosan complex formed prior to the nucleation of the particles. Indeed, the formation of Fe-chitosan complex positively interferes in the crystal growth process by controlling the iron ions diffusion, leading to the formation of crystals with a narrow size distribution and small diameter (Wang et al., 2009).

TEM analysis of ChM 0.05 sample (reference sample, once it has shown better results) at different amplifications is shown in Fig. 2(b) and (c). Despite nanoparticles were agglomerated during the briefly drying process, a reasonable homogenization with a narrow size distribution was noticed, also showing a spheroidal morphology. Instead, chitosan layer was not visible in these images, owing to low contrast of chitosan on the grid. Fig. 2(b) shows the corresponding histogram (inset). The size distribution was also determined using an image analysis program from different micrographs. As it can be seen, the diameter of the nanoparticles ranges from 10 to 25 nm, smaller than magnetic nanocomposites prepared by conventional co-precipitation described in the literature (Li, Jia, Zhou, Hu, & Cai, 2006; Yallapu et al., 2011). Shete and coworkers also obtained chitosan-based materials with particle size about 15 nm (Shete et al., 2014). Other authors, using *in situ* synthesis, reported diameter values even smaller than those obtained in this method (Gregorio-Jauregui et al., 2012; Wang et al., 2009), but it cannot be excluded that in this ultrasound assisted method the oxidation of magnetite may decrease, once the procedure is carrying out in ~2 min. For comparison, values calculated by TEM were similar to particles size estimated by Scherrer's equation (2).

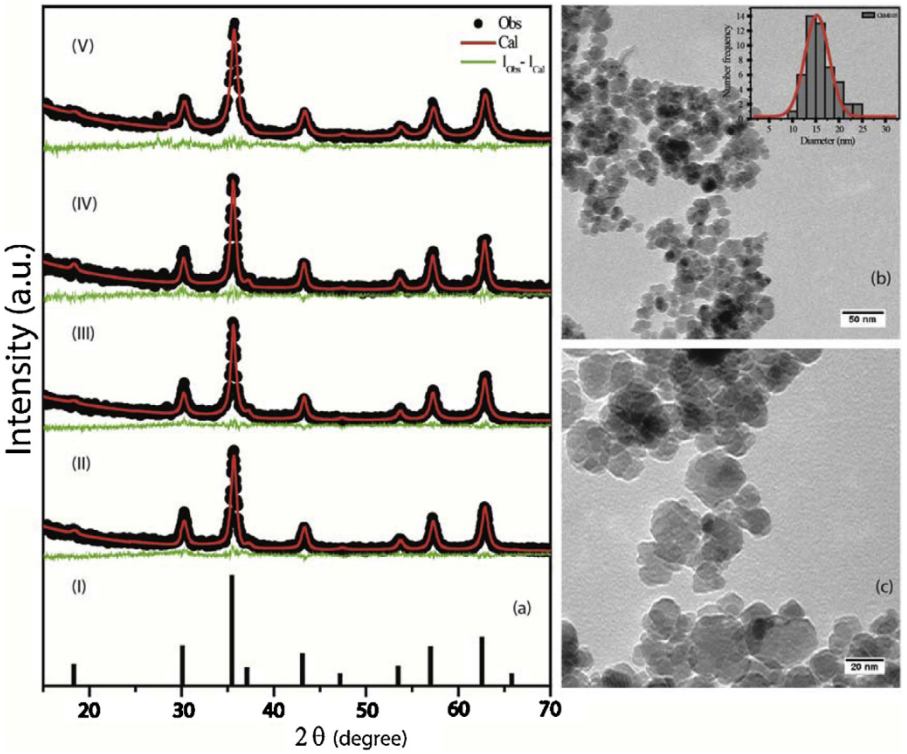

Fig. 2. (a) XRPD patterns of the (I) standard Fe_3O_4 (ICSD, file n° 01-086-1340), (II) Fe_3O_4, (III) ChM 0.01, (IV) ChM 0.05 and (V) ChM 0.1; (b) and (c) TEM images of the sample ChM 0.05 at different amplifications and particles diameter histogram (inset).

Fig. 3(a) shows FTIR spectra to Fe_3O_4, chitosan, and ChM-NPs synthesized with different chitosan amounts. For Fe_3O_4 and nanocomposites, bands around 580 cm^{-1} were assigned to Fe–O deformation in octahedral and tetrahedral sites, confirming the presence of Fe_3O_4 into nanocomposites structure (Donadel et al., 2008). Absorption related to stretching vibration C—O of ether and primary alcohol in the chitosan spectrum was observed in 1027 and 1085 cm^{-1}, respectively. Interestingly, these bands were shifted to 1031 and 1068 cm^{-1} in nanocomposites spectra, where was also observed bands at 1629, 1631 and 1635 cm^{-1}, which can be associated to the stretching of the linking C=N of the imine (Schiff base) from the crosslinked reaction (Kim, Shin, Spinks, Kim, & Kim, 2005). Additionally, the absorption band at 1151 cm^{-1} is characteristic of the asymmetric stretching of C—O—C bridge (Kyzas & Lazaridis, 2009). In chitosan spectrum, an absorption at 1658 cm^{-1} was also observed, corresponding to stretching C=O of amide group (Donadel et al., 2008). The same band in nanocomposites spectra cannot be observed, owing to overlap on the absorption of the C=N imine. In ChM NPs spectra, the absorption around 3452 cm^{-1}, referring to the stretching of chelated OH groups, was overlapped on the stretching of the N—H amine group. However, ChM 0.1 sample showed a band at 1563 cm^{-1} corresponding to the angular deformation of the linking N—H from amine. In chitosan spectrum, the same band was also observed, but shifted to a region of lower wavenumber. According to Gregorio-Jauregui and coworkers, could be concluded that all chitosan in nanocomposites structures are chemically bounded to the magnetite, since the ChM NPs were washed several times and separated by magnetic decantation (Gregorio-Jauregui et al., 2012).

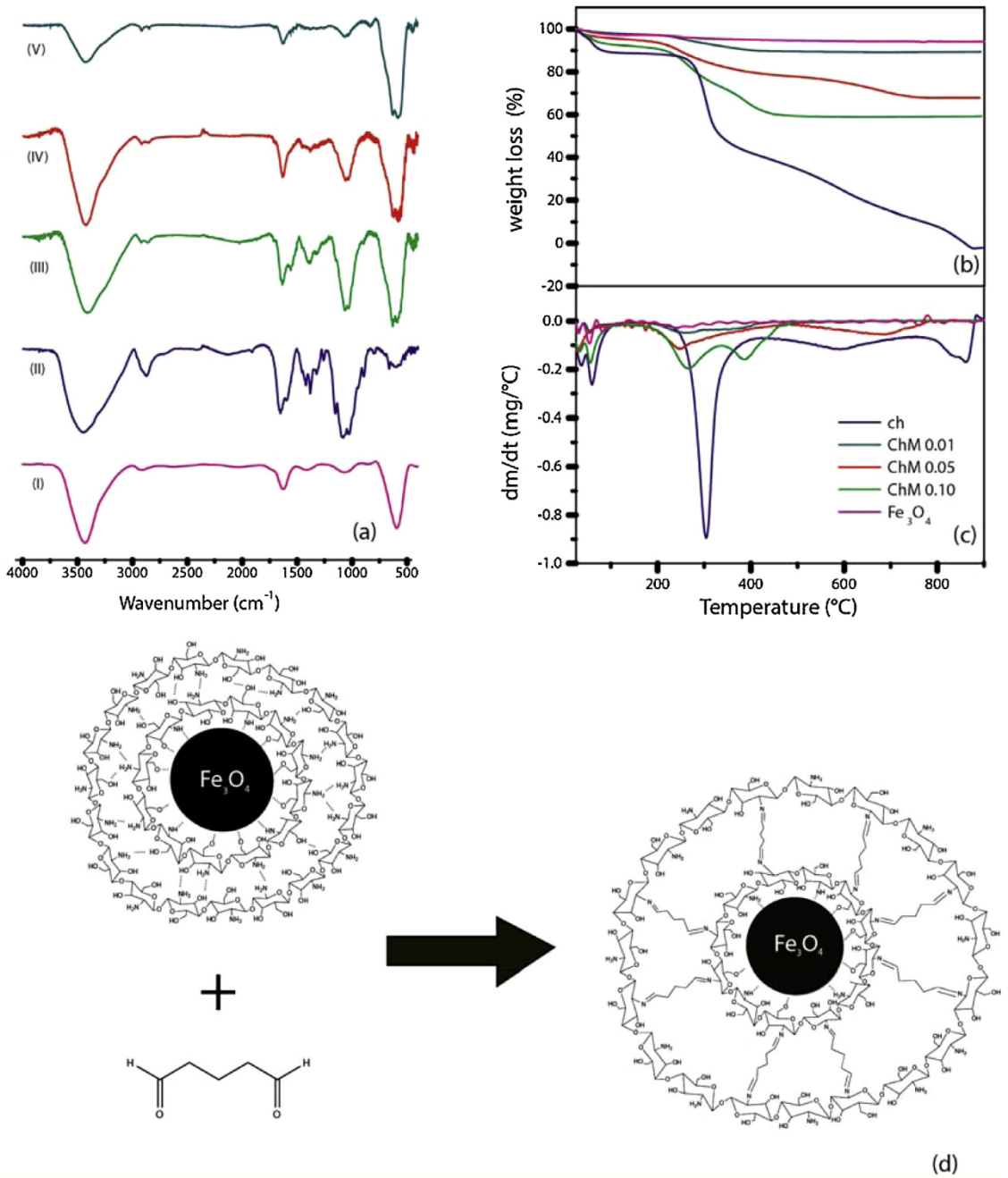

Fig. 3. (a) FTIR spectra of the samples (I) Fe_3O_4, (II) chitosan, (III) ChM 0.1, (IV) ChM 0.05 and (V) ChM 0.01; (b) and (c) TG and DTG curves of the samples Ch (chitosan), ChM 0.01, 0.05 and 0.10, and Fe_3O_4; (d) Illustration of the crosslinking reaction into ChMNP with glutaraldehyde.